

Bethe phase including proton excitations

V. A. Khoze,^{1,2} A. D. Martin¹,, and M. G. Ryskin^{1,2}

¹*Institute for Particle Physics Phenomenology, University of Durham, Durham DH1 3LE, United Kingdom*

²*Petersburg Nuclear Physics Institute, NRC Kurchatov Institute, Gatchina, St. Petersburg 188300, Russia*



(Received 15 October 2019; published 30 January 2020)

We evaluate the contribution of inelastic intermediate states (such as $p \rightarrow N^*$ excitations) to the phase between the one-photon-exchange and the “nuclear” high energy pp scattering amplitudes as $t \rightarrow 0$, caused by multiphoton diagrams. It turns out to be rather small—much smaller than to have any influence on the experimental accuracy of the measurements of ρ , defined to be the ratio of the real to imaginary parts of the forward nuclear amplitude.

DOI: [10.1103/PhysRevD.101.016018](https://doi.org/10.1103/PhysRevD.101.016018)

I. INTRODUCTION

The conventional way to measure the real part of the strong interaction (nuclear) forward amplitude, F^N , is to consider its interference with the pure real one-photon-exchange QED amplitude, F^C , at very small momentum transfer $t \rightarrow 0$. However this interference is affected by the possibility of multiphoton exchange processes which result in an additional phase difference $\alpha\phi$. That is, the total amplitude reads

$$F^{TOT} = F^N + e^{i\alpha\phi} F^C. \quad (1)$$

Here $\alpha = \alpha^{\text{QED}} = 1/137$. The phase ϕ (the so-called Bethe phase) was calculated first by Bethe [1] using a WKB approach, and then was reexamined by West and Yennie [2] in terms of Feynman diagrams. A more precise calculation, which accounts for the details of the proton form factor, was performed by Cahn [3]. It gives

$$\phi(t) = -[\ln(-Bt/2) + \gamma_E + C], \quad (2)$$

where B is the t -slope of the elastic cross section ($d\sigma_{\text{el}}/dt \propto e^{Bt}$), $\gamma_E = 0.577\dots$ is Euler’s constant and $C = 0.62$ (0.60) depending on which form of the proton electromagnetic form factor—exponential (or dipole)¹ is used (see also [4] for a more detailed calculation).

¹Note that the value of $C = 0.62$ (0.60) was calculated in [3] for the ISR energies, assuming $B = 13 \text{ GeV}^{-2}$. In the LHC case with $B = 20 \text{ GeV}^{-2}$ we get $C = 0.45$.

Published by the American Physical Society under the terms of the Creative Commons Attribution 4.0 International license. Further distribution of this work must maintain attribution to the author(s) and the published article’s title, journal citation, and DOI. Funded by SCOAP³.

Note that in all previous calculations only the pure eikonal diagrams were considered. That is only the “elastic” ($p \rightarrow p$) intermediate states were allowed in the multiphoton exchange diagrams Fig. 1(a,b).² Besides this, there are diagrams with the proton excitations shown in Fig. 1(c,d). Of course, at small t due to gauge invariance the $p + \gamma \rightarrow N^*$ vertex contains transverse momentum $q_{T\gamma}$. Therefore, these diagrams do not generate $\ln|t|$ and can only affect the value of the constant C .

In the case of the TOTEM experiment at $\sqrt{s} = 13 \text{ TeV}$ the value of ρ was extracted by fitting the differential $d\sigma_{\text{el}}/dt$ proton-proton elastic cross section in the region of very small $|t| \sim 0.001\text{--}0.005 \text{ GeV}^2$, where the role of the Bethe phase is not negligible. It changes the resulting value of $\rho \equiv \text{Re}/\text{Im}$ ratio by about 0.03. This should be compared with the experimental accuracy 0.01 ($\rho = 0.10 \pm 0.01$ [5]). However, the variation of C by $\delta C = O(1)$ may additionally shift the value of ρ by $\delta\rho = 0.01\text{--}0.02$. Such an effect could potentially be important for the confirmation of the possible presence of the odd signature (Odderon) contribution in the high energy pp -amplitude at $t \rightarrow 0$. Indeed the value of $\rho = 0.10 \pm 0.01$, extracted using the phase ϕ calculated in [3] (without accounting for the possibility of proton excitation) is noticeably lower than that ($\rho \simeq 0.135$) obtained from dispersion relations for a pure even-signature amplitude (with the total cross sections measured by TOTEM). The observed difference $0.135 - 0.10 = 0.035 \pm 0.01$ can be explained either by the odd-signature nuclear contribution to elastic pp scattering or by a modification of the constant C due to the diagrams of Figs. 1(c,d) with inelastic ($p \rightarrow N^*$) intermediate states.

Therefore, it is timely to evaluate the possible role of the processes with proton excitations in the Coulomb-nuclear

²Actually working at $O(\alpha)$ accuracy it is sufficient to study only the two-photon exchange QED diagram and one additional photon in the nuclear amplitude.

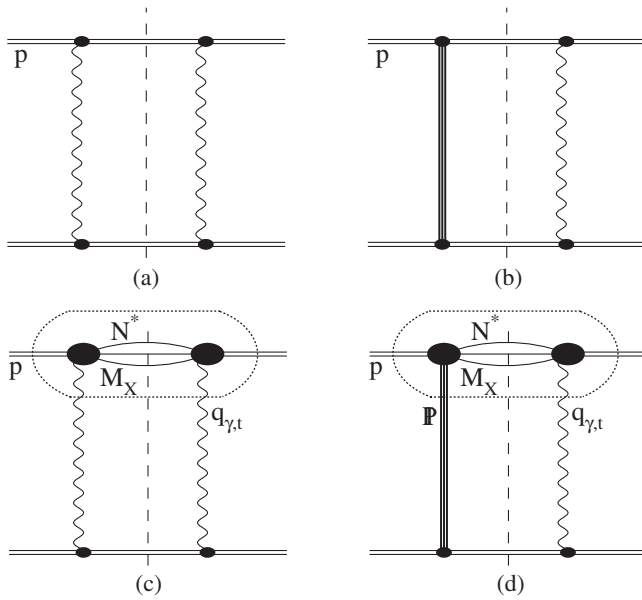


FIG. 1. Diagrams responsible for the Bethe phase at the lowest α^{QED} order. The four plots are: (a) the eikonal (elastic) phase of the one-photon-exchange amplitude, (b) the elastic phase of the strong interaction amplitude, (c) and (d) are the contributions of the excited ($p \rightarrow N^*$) intermediate states. The nuclear amplitude is shown by the triple solid line and marked as \mathbb{P} .

interference region. Unfortunately, there are no sufficient data on diffractive $p \rightarrow N^*$ dissociation which would allow the calculation of the contribution of Fig. 1(d) explicitly. On the other hand, it is known that cross section of low-mass diffractive excitation is well described by the so-called Deck $p \rightarrow N + \pi$ process [6], shown in Fig. 2(a).

Therefore, in Sec. II we use the diagrams of Fig. 2(a) to evaluate the expected shift δC caused by low-mass excitations. The higher-mass contribution is calculated in Sec. III based on the triple-Regge formalism [Fig. 2(b)] and duality. Next, in Sec. IV, we calculate the phase shift $\delta\phi^C$ originating from the two-photon graph Fig. 1(c). Here data on the γp cross sections are available and will be used. Unlike one-photon exchange this diagram does not contain

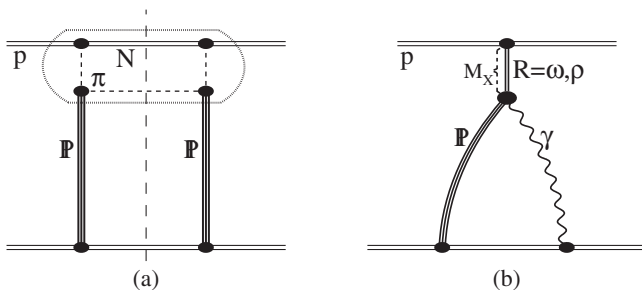


FIG. 2. (a) The Deck diagram for low-mass proton dissociation. (b) The diagram of triple-Regge form used to evaluate, via duality, the contribution of the heavier intermediate states.

a factor of $1/t$. Thus, at very small $t \rightarrow 0$ the corresponding correction is strongly suppressed and can be neglected. Besides this, formally the diagram in Fig. 1(c) describes the even-signature amplitude and should satisfy even-signature dispersion relations. We conclude in Sec. V.

II. PHASE SHIFT CAUSED BY THE DECK PROCESS

At the lowest α^{QED} order the phase of the strong interaction amplitude (marked in figures as \mathbb{P}) is given by the *discontinuity* shown in Figs. 1(b,d) by the vertical dashed lines. Taking the discontinuity of the amplitude, that is replacing $i\pi$ by $2i\pi$ in the imaginary part of the propagator we account for the contribution where the photon exchange is now placed to the left of the nuclear amplitude. Besides this, in Fig. 1(d) (and also in Figs. 3 and 4) we have to include an additional factor of 2 since the lower proton can also dissociate. Instead of the $p \rightarrow N^*$ low-mass excitation we consider the simplest diagrams for the $p \rightarrow N\pi$ transition which rather well reproduce the low-mass proton dissociation [6]. In particular, the cross section of diffractive dissociation calculated via the diagram of Fig. 2(a) at the LHC energy $\sqrt{s} = 7$ GeV is about 2.7 mb (for dissociation of both—that is either the upper or lower—protons). This is close to the value of low-mass dissociation ($\sigma^{\text{SD}}(M_X < 3.4 \text{ GeV}) = 2.66 \pm 2.17 \text{ mb}$) measured by TOTEM [7] (see also the discussion in sect. 3 of [8]).

Recall that the amplitude of the Deck processes is described by *three* diagrams shown in Fig. 3. For the photon exchange amplitude we have an analogous set of

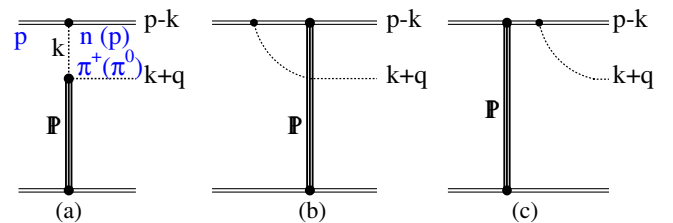


FIG. 3. The nuclear “Deck” amplitudes for low-mass proton dissociation.

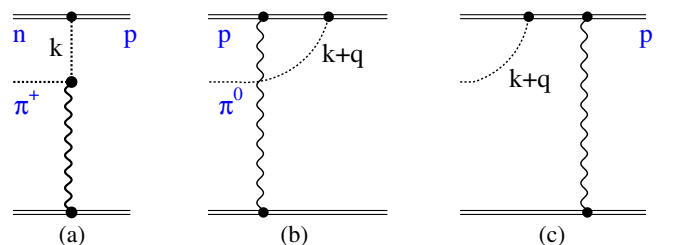


FIG. 4. The QED Deck amplitudes for low-mass proton dissociation.

three diagrams (Fig. 4). That is, to calculate the discontinuity we have to sum up the three diagrams of Fig. 3 and multiply this contribution by the sum of the three diagrams of Fig. 4.

Since we are looking just for an additional Bethe phase which may affect the $\rho = \text{Re}/\text{Im}$ ratio we should not worry about an exact value of the high energy strong amplitude. We use the normalization $s\sigma_{\text{tot}} = \text{Im}T(t=0)$ assuming that $\sigma_{\text{tot}} \propto s^{0.1}$ and use the additive quark model relation $\sigma(\pi p) = (2/3)\sigma(pp)$.

First, the amplitude shown in Fig. 3(a) reads

$$\begin{aligned} A^{3a} &= G_{\pi N} G(k^2) \frac{\sqrt{-k^2}}{k^2 - m_\pi^2} T_{\pi p}(xs, t) \\ &= G_{\pi N} G(k^2) \frac{\sqrt{-k^2}}{k^2 - m_\pi^2} i(1 - i\rho) \\ &\quad \times xs \frac{2}{3} \sigma_0 \left(\frac{xs}{s_0} \right)^{\alpha_p(t)-1} F_\pi(t) F_p(t), \end{aligned} \quad (3)$$

where x is the beam momentum fraction carried by the pion, s is the initial energy squared and $T_{\pi p}$ is the amplitude of the strong πp interaction parametrized in the final equality of the above equation by the pomeron pole exchange with effective trajectory $\alpha_p(t) = 1 + \Delta + \alpha'_p t$, with $\text{Im}T_{pp}(s) = s\sigma_0(s/s_0)^{\alpha_p(0)-1}$, in which we take $\Delta = 0.1$ and $\alpha'_p = 0.25 \text{ GeV}^2$. As usual $s_0 = 1 \text{ GeV}^2$. The coupling $G_{\pi N} = G_{\pi N}(k^2 = 0)$ for the γ_5 proton pion vertex³ is $G_{\pi^0 pp}^2/4\pi = 13.75$ [9] at $k^2 = 0$ with the dipole form factor

$$G(k^2) = 1/(1 - k^2/0.71 \text{ GeV}^2)^2. \quad (4)$$

m_π is the pion mass, and we will take m to be the mass of the proton.

Besides the contribution from the term $\alpha'_p t = \alpha'_p q^2$, the $q^2 = t$ dependence of the strong amplitude is driven by the ‘‘form factors’’ in the vertices

$$F_p(q^2) = 1/(1 - q^2/0.71 \text{ GeV}^2)^2, \quad (5)$$

$$F_\pi(q^2) = 1/(1 - q^2/0.6 \text{ GeV}^2). \quad (6)$$

Analogously, the amplitudes corresponding to Figs. 3(b,c) are

$$\begin{aligned} A^{3b} &= G_{\pi N} G(k^2) \frac{\sqrt{-k^2}}{(p - k - q)^2 - m^2} i(1 - i\rho) \\ &\quad \times (1 - x) s \sigma_0 \left(\frac{(1 - x)s}{s_0} \right)^{\alpha_p(q^2)-1} F_p^2(q^2), \end{aligned} \quad (7)$$

and

³For π^+ the coupling is $\sqrt{2}$ larger than for π^0 .

$$\begin{aligned} A^{3c} &= G_{\pi N} G(k^2) \frac{\sqrt{-k^2}}{(p + q)^2 - m^2} \\ &\quad \times i(1 - i\rho) s \sigma_0 \left(\frac{s}{s_0} \right)^{\alpha_p(q^2)-1} F_p^2(q^2). \end{aligned} \quad (8)$$

For completeness we give the formulas for the propagators:

$$\begin{aligned} k^2 - m_\pi^2 &= -\frac{1}{1 - x} (k_t^2 + x^2 m^2) - m_\pi^2, \\ (p + q)^2 - m^2 &= \Delta M^2 \\ (p - k - q)^2 - m^2 &= m_\pi^2 - k^2 - q_t^2 - \Delta M^2, \end{aligned} \quad (9)$$

where

$$\Delta M^2 = (m^2 + q_t^2)/(1 - x) + (m_\pi^2 + (k + q_t)^2)/x - m^2. \quad (10)$$

Note that here the values of k_t^2 , q_t^2 and $(k + q_t)^2$ are positive. At very high energies $s \gg q_t^2$ where the photon virtuality $q^2 = -q_t^2$.

The QED amplitudes of Fig. 4 take the form

$$A^{4a} = G_{\pi N} G(k^2) \frac{\sqrt{-k^2}}{k^2 - m_\pi^2} \frac{8\pi\alpha}{q^2} xs F_\pi(q^2) F_p(q^2), \quad (11)$$

$$A^{4b} = G_{\pi N} G(k^2) \frac{\sqrt{-k^2}}{(p - k - q)^2 - m^2} \frac{8\pi\alpha}{q^2} (1 - x) s F_p^2(q^2), \quad (12)$$

and

$$A^{4c} = G_{\pi N} G(k^2) \frac{\sqrt{-k^2}}{(p + q)^2 - m^2} \frac{8\pi\alpha}{q^2} s F_p^2(q^2). \quad (13)$$

Again a dipole form factor

$$F_p = F_{p\gamma}(q^2) = 1/(1 - q^2/0.71 \text{ GeV}^2)^2 \quad (14)$$

is used for the photon-proton vertices while for the pion-photon coupling we take the pole form

$$F_\pi = F_{\pi\gamma}(q^2) = 1/(1 - q^2/0.6 \text{ GeV}^2). \quad (15)$$

Recall that for the case of π^+ the coupling $G_{\pi N}$ must be multiplied by $\sqrt{2}$ and we have to deal with the sum $A^{4a} + A^{4c}$ while the total QED amplitude with a π^0 meson is given by $A^{4b} + A^{4c}$. It is easy to check that the total QED amplitude of proton excitation vanishes as $q_t \rightarrow 0$.

The product of the total nuclear times the total QED amplitudes now has to be integrated over the momentum fraction x and the transverse momenta q_t and k_t . Recall that we are seeking for the phase ϕ at $t = 0$. We find

$$\alpha\phi^{\text{Deck}} = \frac{2}{32\pi^2 s^2 \sigma(pp)} \int_0^1 \frac{dx}{x(1-x)} \times \int dq_t^2 \int d^2k_t (\text{Im}A^{(3)}) \cdot A^{(4)}, \quad (16)$$

where $A^{(3)}$ and $A^{(4)}$ denote the total amplitudes, that is the sum of the corresponding a, b, c contributions. The factor 2 accounts for the dissociation of the lower proton. The denominator in $dx/(x(1-x))$ arises from the $1/(2E_\pi 2E_N)$ factors in the phase space integrals $d^3k/(2E(2\pi)^3)$.

Numerical calculation at $\sqrt{s} = 13$ TeV results in $\alpha\phi^{\text{Deck}} = 1.3 \times 10^{-4}$, which is negligibly small in comparison with the experimental accuracy of 0.01. In terms of the Bethe phase, the ‘‘inelastic’’ diagrams with proton low-mass excitations change ϕ by about 0.018.⁴ A similar variation (0.02) of ϕ was observed in [3] depending on the form of the parametrization of the ‘‘elastic’’ proton form factor—that is either dipole or exponent).

A. Deck cross section

The cross section of low-mass dissociation given by the Deck diagram shown in Fig. 2(a) reads

$$\sigma^{\text{SD}} = \frac{1}{4s^2 \cdot (4\pi)^3} \int_0^1 \frac{dx}{x(1-x)} \int dq_t^2 \int dk_t^2 A^{(3)} \cdot A^{*(3)}. \quad (17)$$

Here we account for the dissociation of only one of the colliding proton. For $\sqrt{s} = 7$ TeV we note that the total cross section⁵ $\sigma_{\text{tot}} = 97$ mb and (17) gives $\sigma^{\text{SD}} = 1.35$ mb. This is to be compared with low-mass dissociation cross section $2.6/2 = 1.3 \pm 1.1$ mb observed by TOTEM [7]. The good agreement confirms the applicability of our calculation of the low-mass proton excitation contribution to the Bethe phase ϕ .

III. HIGHER-MASS DISSOCIATION

To evaluate the possible role of higher-mass excitations we consider the ‘‘triple-Regge’’-like diagram of Fig. 2(b). Since the $RP\gamma$ triple vertex is not known

⁴The reason for such a small contribution from proton dissociation is as follows. The low-mass nucleon photo-excitation is mainly a magnetic transition which flips the proton helicity. Indeed, the spin flip in $N \rightarrow N^*$ transition is needed in order to compensate for the spin = 1 of γ quantum in the $N^* \rightarrow p\gamma$ decay. On the other hand, the Pomeron exchange amplitude contains two components: one conserving the s -channel helicity and another one which flips the helicity. The second component acts as the anomalous magnetic moment. Let us assume that the Pomeron-nucleon vertex is similar to the photon-nuclear vertex [10]. Then the term responsible for the spin flip component is given by the anomalous magnetic moment for zero isospin ($I = 0$) exchange amplitude. That is for the diffractive transition $\mu_{I=0} = (\mu_p + \mu_n)/2 = (1.79 - 1.91)/2 = 0.06$ is very small.

⁵This is the value between the cross sections given by TOTEM [11] and by ATLAS-ALFA [12].

phenomenologically we use the ‘‘vector dominance model’’ (VDM) [13] approach and replace this vertex by the ‘‘Pomeron— ρ -meson’’ (or ω -meson) vertex which in its turn can be written as 2/3 of the Pomeron-proton vertex. Recall that due to gauge invariance the proton excitation vertex caused by the photon must vanish as $q^2 \rightarrow 0$. The dimension of the corresponding q^2 factor should be compensated either by the radius of the $RP\gamma$ triple vertex or by the mass difference $\Delta M^2 = M^2 - m^2$. In the present calculation we use $s_0 = 1$ GeV². On the one hand, this simplifies the final Regge formula, while on the other hand this is close to the expected size of the vertex driven by the slope of the R -reggeon (ρ, ω) trajectory $\alpha'_R = 0.9$ GeV⁻² [14].

Next, it is known within the VDM, that the proton-to-photon coupling (proton electric charge e) can be considered as the sum of the contributions mediated by the ρ and ω mesons. Exploiting the fact that the ρ and ω Regge trajectories are degenerate [14] we calculate the contribution shown in Fig. 2(b) as

$$\alpha\phi^R = \alpha'_R \pi \frac{2\alpha}{3\pi} \int \frac{dM_X^2}{M_X^2} \left(\frac{M_X^2}{s_0}\right)^{\alpha_R(0) - \alpha_P(0)} \times \int dq_t^2 F_p^2(q^2) \left(\frac{M_X^2}{s}\right)^{\alpha_P q^2}. \quad (18)$$

Here M_X is the mass of the proton-excited system described by the R -reggeon and we have already accounted for the possibility of excitation of the lower proton.

The first factor $\alpha'_R \pi$ in (18) accounts for the relation between the imaginary part of the Reggeon exchange amplitude given by the R -Reggeon signature factor

$$\eta = \frac{1 - \exp(-i\pi\alpha_R(t))}{\sin(-\pi\alpha_R(t))} \quad (19)$$

and the residue of the pole at $\alpha_R(t) = 1$. Near the pole the signature factor (19) takes the form $2/(\alpha'_R \pi(t - m_R^2))$ while the discontinuity at $t = 0$ (where $\alpha_R(0) \simeq 1/2$) is $2\text{Im}\eta \simeq 2$.

The numerical calculation of (18) results in

$$\phi^R = 0.099 - 0.106 \quad (20)$$

for $\alpha_R(0) = 0.5 - 0.54$. This leads to a correction

$$\alpha\phi^R \simeq 0.0007 - 0.0008 \quad (21)$$

to the $\rho = \text{Re}/\text{Im}$ ratio for the ‘nuclear’ amplitude.

Recall that for this evaluation we used a very approximate approach. Nevertheless, the result is an order-of-magnitude less than the accuracy of the present experiment (see [5]). Moreover, most probably the true value of ϕ^R is even smaller since, as a rule, the triple-Reggeon vertices

extracted from the phenomenological triple-Regge analysis are smaller than the corresponding Reggeon-hadron vertices (see for example [15], and the discussion below).

In terms of VDM the interaction with the photon starts from the transition of a pointlike photon to the $q\bar{q}$ pair where the quark-quark separation, r , is close to zero. On the other hand the Pomeron-induced cross section of such a pair behaves as $\sigma \propto \alpha_s^2 \langle r^2 \rangle$ [16]. Most probably the time interval occupied by the $RP\gamma$ interaction is not sufficient to form the ρ - or ω - mesons in their normal (equilibrium) states, so the resulting values of r^2 , which drive the value of the vertex, will be smaller than that used in our estimate (based on the assumption that $\sigma_{pR} = \sigma_{\omega p} = (2/3)\sigma_{pp}$). This qualitatively explains why we expect that the value of ϕ^R to be smaller than that calculated above.

Note also that strictly speaking one should not sum the phases ϕ^{Deck} and ϕ^R . This will lead to double counting since when calculating ϕ^R using (18) we integrate over M_X starting from $M_X = s_0 = 1 \text{ GeV}^2$. If we would like to keep the contribution described by the Deck diagrams then in (18) we have to take a larger lower limit for M_X . This will diminish the value of ϕ^R .

IV. TWO-PHOTON EXCHANGE WITH PROTON EXCITATION

The inelastic contribution of the two-photon exchange diagram shown in Fig. 1(c) can be calculated using the equivalent photon approximation [17]. The imaginary part of the amplitude in Fig. 1(c) reads

$$A^{1c} = 2 \frac{\alpha}{\pi^2} s \int \frac{dE_\gamma}{E_\gamma} \int d^2 q_t \frac{(q_1 \cdot q_2)}{q_1^2 q_2^2} \sigma_{\gamma p}^{\text{tot}}(E_\gamma) F_p(q_1^2) F_p(q_2^2), \quad (22)$$

where first factor 2 accounts for the excitations of the second [lower in Fig. 1(c)] proton. Here we have to be more precise and to account for the small but nonzero total momentum transferred $t = Q^2 = -Q_t^2$. The momenta of the “left” and the “right” photons in Fig. 1(c) are

$$q_{1,2} = q_t \pm \frac{Q_t}{2} \quad (23)$$

and $(q_1 \cdot q_2)$ denotes the scalar product of q_1 and q_2 . E_γ is the photon energy in the upper [in Fig. 1(c)] proton rest frame; $\sigma_{\gamma p}^{\text{tot}}$ is the total cross section of photon-proton interaction.

The resulting value of A^{1c} in (22) should be compared with the one-photon exchange (Coulomb) amplitude (which is real)

$$F^C(t) = s \frac{8\pi\alpha}{Q^2}. \quad (24)$$

Note that, contrary to F^C , the proton excitation contribution A^{1c} of (22) does not contain a $1/Q^2$ pole. Therefore, the phase generated by the A^{1c}/F^C ratio vanishes at $t = Q^2 \rightarrow 0$. However actually the Coulomb-nuclear interference is measured at $|t| \sim 0.001 \text{ GeV}^2 \neq 0$. That is why we wrote the formula (22) accounting for the value of Q_t .

For the numerical estimate we take the experimentally measured $\sigma_{\gamma p}^{\text{tot}}(E_\gamma)$ cross sections [18,19] at $E_\gamma = 0.26\text{--}4.2 \text{ GeV}$. For a larger $E_\gamma > 4 \text{ GeV}$ we use parametrization of [18]

$$\sigma_{\gamma p}^{\text{tot}}(E_\gamma) = (91 + 71.4/\sqrt{E_\gamma})\mu\text{b} \quad (25)$$

with E_γ in GeV. In this parametrization we keep only the second term since the first term corresponds to Pomeron exchange ($\sigma = \text{const}$) and should be treated as an $O(\alpha^2)$ correction to the strong interaction (even-signature) amplitude.

As seen from Fig. 5, in the region of interest ($|t| < 0.001\text{--}0.005 \text{ GeV}^2$), where Coulomb-nuclear interference manifests itself, the possibility of proton excitations in the two-photon exchange process changes the original phase of the pure QED one-photon-exchange amplitude by the negligibly small value of $|\delta\phi^C| < 10^{-3}$.

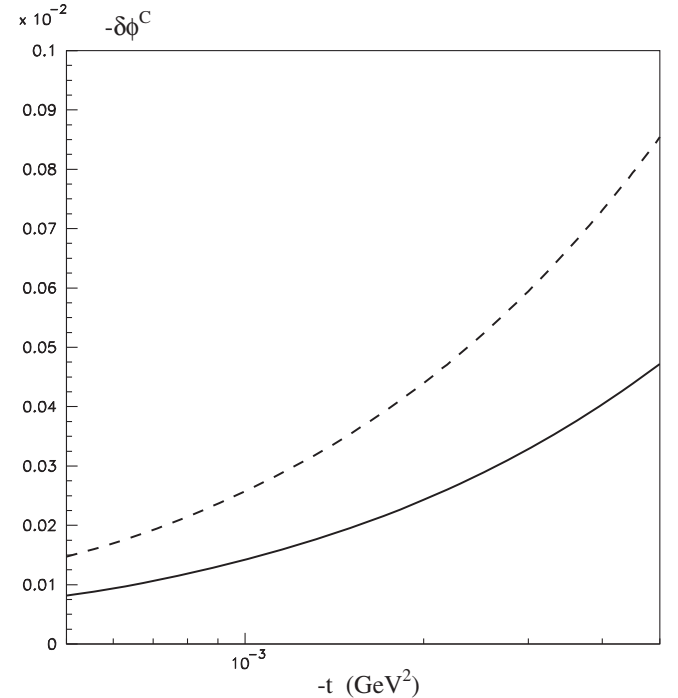


FIG. 5. The phase shift $\delta\phi^C$ of the one-photon-exchange amplitude caused by the second photon exchange with proton excitations in the intermediate states. The dashed line is calculated using the full photon-proton cross section, $\sigma_{\gamma p}^{\text{tot}}(E_\gamma)$ at $E_\gamma < 4.2 \text{ GeV}$, while for the solid curve the Pomeron (constant) “background” of $91 \mu\text{b}$ was subtracted from $\sigma_{\gamma p}^{\text{tot}}$.

V. CONCLUSION

We evaluated the contribution of proton ($p \rightarrow N^*$) excitations to the phase shift (Bethe phase) between the strong interaction and the one-photon exchange QED amplitudes caused by an additional photon exchange. The low-mass part was calculated based on the Deck [6] ($p \rightarrow N\pi$) mechanism, while the higher-mass excitation was estimated using the triple-Regge formalism. The “inelastic” two-photon exchange QED contribution was calculated using the experimental data on the proton-photon cross section in terms of the equivalent photon approach.

It is shown that the effects are very small and do not change the value of $\rho = \text{Re}/\text{Im}$ ratio, measured via the Coulomb-nuclear interference in small angle elastic pp scattering, by more than $\delta\rho \sim 10^{-3}$. This is about an order-of-magnitude less than the experimental accuracy of ± 0.01 [5].

ACKNOWLEDGMENTS

We thank Per Grafstrom for the interest to our work and useful comments. M. G. R. thanks the Institute for Particle Physics Phenomenology (IPPP) at the University of Durham for hospitality.

-
- [1] H. A. Bethe, *Ann. Phys. (N.Y.)* **3**, 190 (1958).
 - [2] G. B. West and D. R. Yennie, *Phys. Rev.* **172**, 1413 (1968).
 - [3] R. Cahn, *Z. Phys. C* **15**, 253 (1982).
 - [4] O. V. Selyugin, *Phys. Rev. D* **60**, 074028 (1999); *Mod. Phys. Lett. A* **11**, 2317 (1996).
 - [5] G. Antchev *et al.* (TOTEM Collaboration), *Eur. Phys. J. C* **79**, 785 (2019).
 - [6] R. T. Deck, *Phys. Rev. Lett.* **13**, 169 (1964).
 - [7] G. Antchev *et al.* (TOTEM Collaboration), *Europhys. Lett.* **101**, 21003 (2013).
 - [8] V. A. Khoze, A. D. Martin, and M. G. Ryskin, *Phys. Lett. B* **784**, 192 (2018).
 - [9] V. G. J. Stoks, R. Timmermans, and J. J. de Swart, *Phys. Rev. C* **47**, 512 (1993); R. A. Arndt, I. I. Strakovsky, R. L. Workman, and M. M. Pavan, *Phys. Rev. C* **52**, 2120 (1995).
 - [10] P. V. Landshoff and J. C. Polkinghorne, *Nucl. Phys.* **B32**, 541 (1971).
 - [11] G. Antchev *et al.* (TOTEM Collaboration), *Europhys. Lett.* **101**, 21004 (2013).
 - [12] G. Aad *et al.* (ATLAS Collaboration), *Nucl. Phys.* **B889**, 486 (2014).
 - [13] J. J. Sakurai, *Ann. Phys. (N.Y.)* **11**, 1 (1960); T. H. Bauer, R. D. Spital, D. R. Yennie, and F. M. Pipkin, *Rev. Mod. Phys.* **50**, 261 (1978); **51**, 407(E) (1979).
 - [14] A. C. Irving and R. P. Worden, *Phys. Rep.* **34**, 117 (1977); P. D. B. Collins, *An Introduction to Regge Theory and High Energy Physics* (Cambridge University Press, Cambridge, England, 1977).
 - [15] E. G. S. Luna, V. A. Khoze, A. D. Martin, and M. G. Ryskin, *Eur. Phys. J. C* **59**, 1 (2009).
 - [16] G. Bertsch, S. J. Brodsky, A. S. Goldhaber, and J. F. Gunion, *Phys. Rev. Lett.* **47**, 297 (1981); B. Z. Kopeliovich, L. I. Lapidus, and A. B. Zamolodchikov, *Pis'ma Zh. Eksp. Teor. Fiz.* **33**, 612 (1981) [*JETP Lett.* **33**, 595 (1981)].
 - [17] C. Weizsacker, *Z. Phys.* **88** (1934) 612; E. Williams, *Phys. Rev.* **45**, 729 (1934).
 - [18] T. A. Armstrong *et al.* *Phys. Rev. D* **5**, 1640 (1972).
 - [19] M. MacCormick *et al.* *Phys. Rev. C* **53**, 41 (1996).